Proceedings of the ASME 2016 International Mechanical Engineering Congress & Exposition
IMECE 2016
November 11-17, 2016, Phoenix, Arizona, USA

IMECE2016-65298

POWERING A LOWER LIMB EXOSKELETON USING PNEUMATIC ARTIFICIAL MUSCLES

Jonathan M. Chambers
Composites Research Laboratory
Dept. of Aerospace Engineering
University of Maryland
College Park, MD 20742
Email: jmchambe@terpmail.umd.edu

Craig R. Carignan
Space Systems Laboratory
Dept. of Aerospace Engineering
University of Maryland
College Park, MD 20742
Email: craigc@ssl.umd.edu

Norman M. Wereley
Composites Research Laboratory
Dept. of Aerospace Engineering
University of Maryland
College Park, MD 20742
Email: wereley@umd.edu

ABSTRACT

Passive leg exoskeletons are currently being investigated for offsetting the weight of tools and other loads from workers performing maintenance and assembly tasks. By providing power-assist to the knee joints with pneumatic artificial muscles (PAMs), a wider range of stances could be used by maintenance workers without drawing significant power. A simplified kinematic model of the exoskeleton is developed, and the array of potential user stance configurations is then bounded. A static analysis is performed to define the torque required for actuation of the knee joint to support the tool loads carried by the exoskeleton. Finally, an exemplary transmission model is used to verify that it is feasible for a PAM to provide the range of motion and forces required for knee joint actuation. Upon demonstration of the viability of PAM actuation, development of an exoskeleton leg prototype is underway to provide validation of the proposed scheme. The knee actuation system will be retrofit to the FORTIS exoskeleton, and tests on its effectiveness will be conducted.

FIGURE 1. FORTIS EXOSKELETON

1 INTRODUCTION AND BACKGROUND

While the military has largely been focused on developing exoskeletons to give soldiers “ironman”-like capabilities [1], [2], several companies have been investigating this technology to assist workers in more industrial settings. For example, Lockheed-Martin Corp. (LMT) licensed the technology for the Berkeley Bionics Human Universal Load Carrier (HULC) developed for use by soldiers, and stripped it of its actuation to produce a passive exoskeleton intended for manufacturing and maintenance workers. LMT then attached a ZeroG arm [Equipois, Inc.] at the hip of the exoskeleton to support the weight of heavy tools, creating the first MANTIS industrial Human Augmentation System (iHAS). The basic design of the MANTIS was later simplified, and evolved into the FORTIS exoskeleton (Fig. 1).

The U.S Naval Command is currently investigating the deployment of a FORTIS/ZeroG system as a load-bearing device for assisting workers in shipyard and aircraft maintenance tasks to reduce injuries and injury-related costs. Over a three year period, the U.S. Navy reported about 1,000 injuries among shipyard workers ranging from back pains to sprains and tears resulted in over 6,500 lost workdays [3]. Preliminary trials conducted at naval shipyards have shown that the FORTIS was able to offload the weight of machine tools from the user during maintenance tasks resulting in a 70% increase in productivity, a seven-fold increase in task endurance, and a reduction in orthopedic injuries.

The objective of the passive exoskeleton is to help a user support the weight of a tool while performing maintenance and manufacturing tasks. The weight of this load is transferred to the ground through a basic tubular structure that parallels the user's legs. The linkage structure transfers the weight of a load directly to the ground in a straight leg orientation (knee angle = 0°). However, an unsupported torque is expressed at the knee joint with any bent leg orientation. This necessary condition for complete load support can lead the user to exhibit an unnatural stance during tasks, and provides no assistance from a seated position. The overall simplicity of the FORTIS exoskeleton design is commendable, yet the restriction it puts on the number of supported user stances leaves room for improvement. This study addresses this issue with the application of actuated support of the FORTIS knee joint.

Depending on the application, various methods have been employed to support the torque expressed at the knee joint of exoskeletons. Many exoskeletons utilize a passive form of knee support for repetitive or cyclic forms of motion such as walking. Researchers at Yale University applied a passive spring for knee torque assistance during walking after noting that the knee joint acts as a constant force spring during the weight acceptance phase of the gait cycle [4], [5]. The cyclic nature of a person's gait enables the spring to store and release energy in a predictable manner to assist the user. However, with the cyclic loading on the knee dependent on user weight, gait speed, and leg geometry, a different spring must be employed for each individual and circumstance to provide a suitable knee support stiffness. With an infinite number of indiscriminate stances and loads required for our focus of maintenance and manufacturing tasks, the exclusive use of a spring for torque support of the knee is not practical.

Researchers in South Korea considered actuating a knee joint with an electric motor [6]. Electric motors have proven their efficacy in many robotics applications, but they also amount to a heavy design, and fail to provide compliance which aids in providing a more natural feeling human-robot interaction.

Researchers at the University of Brussels developed a powered knee exoskeleton called the KNEXO that utilized an agonist-antagonist pair of pleated PAMs to power a lower limb exoskeleton [7], [8]. Pleated pneumatic actuated muscles provide a high specific force output, and the application of a four-bar transmission scheme maximizes conversion of actuation force to torque throughout the range of motion (ROM) of the knee. However, the employment of pleated PAMs requires large volume changes which creates a bulky form of actuation that requires excessive amounts of pressurized air. Furthermore, the four-bar transmission scheme also adds bulk and complexity to the knee joint that could prove to be problematic in workplaces. The KNEXO is prohibitively bulky and complex for maintenance and manufacturing tasks, but its basic mechanical scheme has motivated the approach taken in this research.

The high specific work output, simple construction, and inherent compliance of pneumatic artificial muscles (PAMs) makes them an ideal form of actuation for exoskeleton applications. Therefore, the goal of this study is to assess the feasibility of supporting the torque expressed at the knee joint through PAM actuation. Most tasks performed by shipyard and aircraft maintenance personnel require them to maintain a fixed stance while supporting the weight of a tool. Therefore, feasibility of the employment of PAM actuation to the FORTIS is determined through a static analysis of the exoskeleton.

The method to test the feasibility of PAM actuation first requires the development of a kinematic model of the FORTIS to characterize the range of feasible user stances. Once the range of feasible stances is bounded, the exoskeleton's loads and required knee torques are characterized for each stance. A simple transmission scheme is implemented to translate the torque requirements into PAM actuator force and displacement requirements. Finally, feasibility of PAM actuation of the FORTIS is determined by comparing the actuation force-displacement required for support of the knee joint, with the force-contraction curves that define the PAM's actuation capabilities.

2 OVERVIEW

The objective is to enable the FORTIS to fully support applied external loads while providing the user with an uninhibited ROM. The user must be capable of situating themselves in any task dependent stance, and have the PAM actuator react to support the full torque expressed at the knee joint.

With the employment of PAM actuation of the knee joint, the PAM's linear contraction motion must be converted to a rotational torque through a transmission mechanism comprised of a pulley, cam, linkage system, or some other conceived means. The selected transmission mechanism and kinematics of the FORTIS dictate both the mechanical advantage and actuation stroke length required of the PAM. These can be translated to force-contraction requirements that the PAM must satisfy to ensure feasibility of the PAM actuated FORTIS concept.

2.1 FORTIS Exoskeleton

The structure of the FORTIS (Fig. 2) is comprised of a central mounting frame and two multi-link legs. The mounting

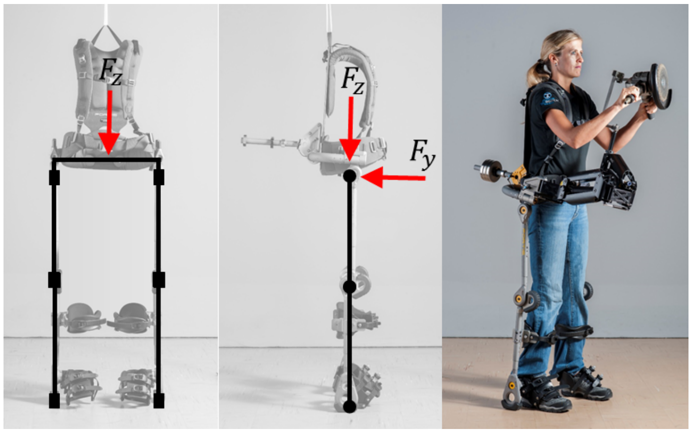

FIGURE 2. FORTIS FRAME VIEWS AND BEING WORN BY SUBJECT.

frame at the user's waist serves as an attachment point for the tool holding arm [ZeroG arm] and a weighted counter-torque appendage. This load is transferred to a pair of two-link legs that each have three revolute joints to provide a total of three DOF for each leg. The two joints at the hip enable hip extension/flexion and abduction/adduction, while a single joint at the knee enables flexion/extension of the knee. The leg linkages also telescope to set heights to enable adjustability for accommodating users of different stature. Footings at the bottom of the lower leg linkage provide a surface to transmit load forces to the ground.

The structure of the FORTIS is attached to the user through adjustable straps at seven points of contact: each calf and foot, around the waist, and over each shoulder. The shoulder straps attach to a back support board that is fixed to the mounting frame, and serves the purpose of counterbalancing the torque applied about the hip from the ZeroG arm. It is undesirable to have any weight supported through the attachment straps. However, a load can be transferred through them to the user from inevitable misalignments between the user and exoskeleton from improper adjustment and fit, or from stances where the footings do not make contact with the ground.

The human versus FORTIS ranges of motion in the hip, knee, and ankle are shown in Table 1. Flexion of the hip for a user is restricted by as much as 30° by the FORTIS. The FORTIS protects against hyperextension of the user's knee by restricting anything past a straight leg orientation (knee angle=0°). Ankle movement is completely unrestricted by the FORTIS which provides a padded footing to accommodate any ankle orientation.

2.2 Pneumatic Artificial Muscles (PAMs)

PAMs are well-suited to this application due to their high specific work, and inherent compliance that aids in the transparency of torque assistance to the user. With the simple construction of an elastomeric bladder, surrounding load-bearing braided sleeve, and two end-fittings, a pressurized PAM can provide a contractile force along its longitudinal axis. With the PAM pressurized, the bladder expands radially against the stiff braided sleeve. This radial expansion causes the sleeve to contract axially, transforming the radial pressure force from the bladder into an axial force transmitted through the sleeve and end fittings.

TABLE 1. FORTIS RANGES OF MOTION.

JOINT	Human [9]	Exoskeleton
hip flex/ext	$110° - 130°/30°$	$100°/30°$
knee flex/ext	$130°/15°$	$130°/0°$
ankle dorsi/plantar	$20°/45°$	$-/-$

Figure 3 illustrates the force-contraction characteristics of a PAM developed at the University of Maryland [10]. A PAM provides a maximum force in a state of zero contraction termed the blocked force, and zero force at a point of maximum contraction termed the free contraction. As evident from the force-contraction curves, the force capabilities of a PAM initially decreases nonlinearly under small contractions ($<$0.025), but then decreases in an approximately linear fashion thereafter. Figure 3 also illustrates how an increase in the applied pressure increases the force output of the PAM. Contraction of a PAM scales linearly with a PAM's resting length, so a PAM fabricated with a longer resting length can provide a larger actuation displacement.

The PAM utilized in this study was constructed of 2.22 cm (7/8 in) outer diameter tubing with a 3.81 cm (1.5 in) outer diameter Kevlar braided sleeve, and has an effective active length of 19.0 cm (7.5 in). The length of this PAM is scaled up to 30.48 cm (12 in) in length to enable an increased magnitude of contraction for this study.

2.3 Design Constraints

Retrofitting the FORTIS imposes constraints on potential actuation and transmission schemes. With the PAM mounted parallel to the thigh link, the thigh link length limits maximum stroke length of the PAM (stroke length scales linearly with PAM resting length). It is also desired to have a transmission scheme that does not consume a large volume around the knee joint in order to not impede the motion of the user. Anything that protrudes outward excessively from the knee can create a hazard in the workplace. Although not a consideration in the current analysis, volume and pressure requirements for PAM actuation can become an additional design requirement for applications without access to a shop air source. Compressed air for the PAM would then need to be carried onboard the exoskeleton. Overall, for optimization of additional design constraints, both PAM sizing and

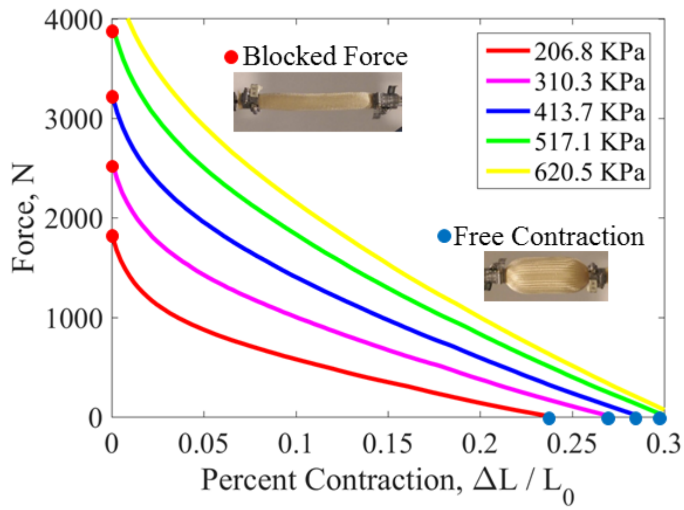

FIGURE 3. PAM FORCE VERSUS PERCENT CONTRACTION FOR A RANGE OF TESTED PRESSURES.

transmission design will need to be revisited.

3 MODELING OF THE FORTIS

A computer model is developed in MATLAB to characterize the kinematics and static loads of the FORTIS. A simple knee joint pulley system is then detailed to serve as an exemplary transmission mechanism. With the realized loads and transmission mechanism, the feasibilty of a PAM actuated FORTIS can then be examined in Section 4.

3.1 Kinematic Model of FORTIS

Figure 4 provides an illustration of the realized model of the FORTIS, while Eqs. (1- 4) present the equations for the position of the knee joints (k) and footings (r) with respect to the hip position h, link lengths L_{thigh} and L_{shank} , and joint angles θ_{hip} and θ_{knee}. Just as with the actual FORTIS, each leg of the model is comprised of joints at the hip and knee connected to two links (thigh and shank). The model has a revolute joint at the knee and hip joint that provide two DOF in the sagittal plane. Abduction/ adduction (coronal plane motion) of the hip is excluded from the model as a simplification of analysis. This simplification is enabled by the fact that the torque expressed on the knee joint (sagittal plane) is perpendicular to the loads in the coronal plane (hip abduction/adduction). Therefore, for a given extension/flexion of the knee and hip joints, variation of the hip angle in the coronal plane would have a minimal effect on the torque expressed at the knee joint of the FORTIS. The ROMs of the joints in the model mirror the values approximated in Table 1 for the user and FORTIS. The kinematic equations tracking the position of the knee (k) and footing (r) are given as:

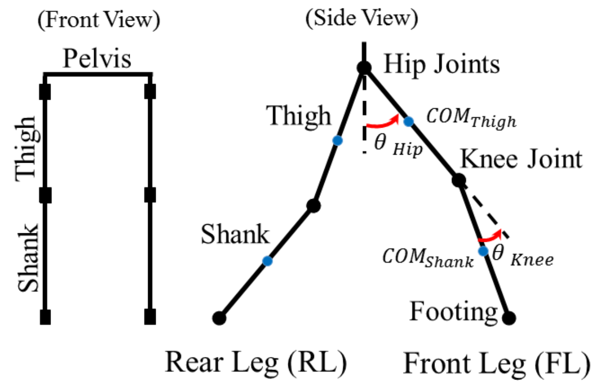

FIGURE 4. FORTIS PLANAR MODEL.

$$k_y = h_y + L_{thigh}\sin(\theta_{hip}) \tag{1}$$
$$k_z = h_z - L_{thigh}\cos(\theta_{hip}) \tag{2}$$
$$r_y = k_y + L_{shank}\sin(\theta_{hip} + \theta_{knee}) \tag{3}$$
$$r_z = k_z - L_{shank}\cos(\theta_{hip} + \theta_{knee}) \tag{4}$$

3.2 Characterization of Feasible Stance Orientations

The forces transferred through each leg are dependent on the proportion of the total load that each leg has to support, and on the joint angles that determine the manner at which loads are transferred from one link to another. Load distribution between each leg is dictated by the footing positions with respect to the position of the tool load (between the hip joints). Because there are an infinite number of leg orientation combinations with respective footing positions for different stances, there are also a countless number of loading scenarios for the exoskeleton. Therefore, an iterative method was developed to reduce the number of possible stances, and delineate the boundaries of possible leg orientations.

Feasible stances and their respective leg orientations are defined as those that obey the following three conditions: orientations that are within the ROM of both the user and FORTIS, orientations that enable both footings to be in contact with the ground, and orientations that provide static stability of the loads on the exoskeleton (governed by the center of mass position with respect to the two footings).

To execute this method, a single leg orientation is locked in place, while the opposing leg is iteratively swept and checked for compliance with the conditions for feasible leg orientations as listed above. Figure 5 provides a depiction of what results from the stated method. First, an orientation of the front leg (FL) is set. Then orientations of the rear leg (RL) are tested against the feasibility conditions while iteratively sweeping the hip angle away

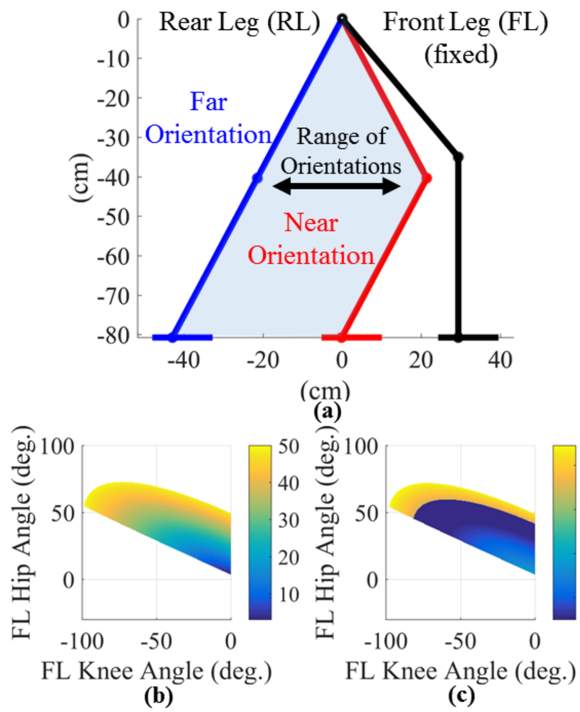

FIGURE 5. (a) DEPICTION OF THE RANGE OF FEASIBLE RL STANCES WITH A SET FL ORIENTATION. RL (b) NEAR AND (c) FAR HIP ORIENTATIONS WITH RESPECT TO EVERY SET FL ORIENTATION (θ_{hip} , θ_{knee})

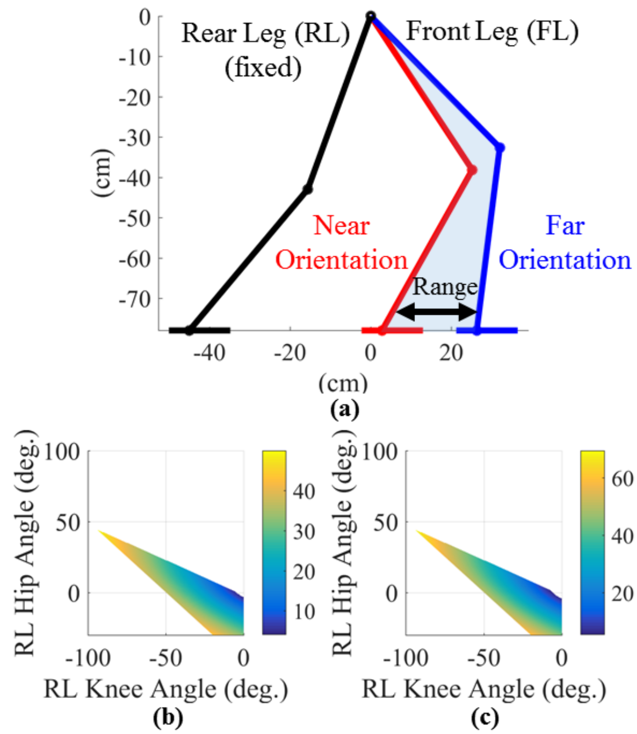

FIGURE 6. (a) DEPICTION OF THE RANGE OF FEASIBLE FL STANCES WITH A SET RL ORIENTATION. FL (b) NEAR AND (c) FAR HIP ORIENTATIONS WITH RESPECT TO EVERY SET RL ORIENTATION (θ_{hip} , θ_{knee})

from the set hip angle of the FL. After the RL hip angle is iterated through every angle within the hip's ROM, what remains is a range of possible RL leg orientations for the set FL orientation. The boundaries of the range of possible RL leg orientations are termed the near orientation and far orientation. This process for the single set FL orientation is then repeated for every FL orientation within the ROM of the hip and knee joints. What results from this procedure is a near and far orientation of the RL for every FL orientation within the leg's ROM. With the static force analysis presented in Section 4.1, the near and far orientations of the RL will be seen to represent the minimum and maximum FL loading conditions respectively for each set FL orientation tested. Figure 6 provides an illustration of the same method repeated for every set RL orientation as was already done for the FL.

Upon the completion of this method, every feasible FL orientation has defined boundaries for the range of feasible RL orientations (near/far orientations), and every RL orientation has defined boundaries for the range of feasible FL orientations.

3.3 Static Force Model

The static equilibrium equations for the FORTIS exoskeleton model developed in the preceding section are now presented. These equations are solved with the goal of finding the torque expressed at the knee joint ($M_{x,knee}$) for static equilibrium in all feasible stances. En route to this goal, the forces on every other joint are also calculated. Forces between the user and exoskeleton (through connecting straps) are not accounted for in this analysis. Ideal fit and operation of the FORTIS would minimize these forces making them inconsequential. However, if forces between the user and structure are appreciable, the user would be supporting loads that would offload the exoskeleton. Therefore, the following analysis yields maximum loads on the structure.

Fig. 7 illustrates all of the external loads that act on the exoskeleton structure in their assumed positive directions with the corresponding equilibrium equations (Eqs. (5- 7)). F_z represents the weight supported at the pelvis (tool, tool holder, counter weight, and structure weight) while F_y is the horizontal response between the tool and a working surface. Any additional inertial or external forces applied to the tool are provided by the user. There are also no moments transmitted through the revolute hip joints. Any torque created by shifting the center of mass (COM) (through movement of the ZeroG arm) is compensated for by the counterweight mounted behind the hip, and by the user through the back support board and shoulder straps. Each leg link has an

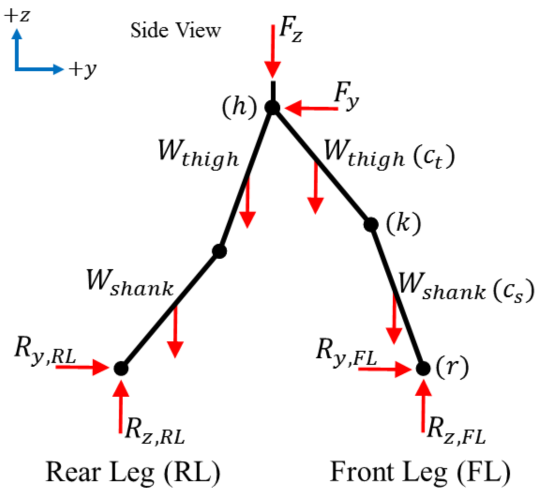

FIGURE 7. EXTERNAL LOADING ON EXOSKELETON SYSTEM. (POSITIONS LABELED IN PARENTHESIS)

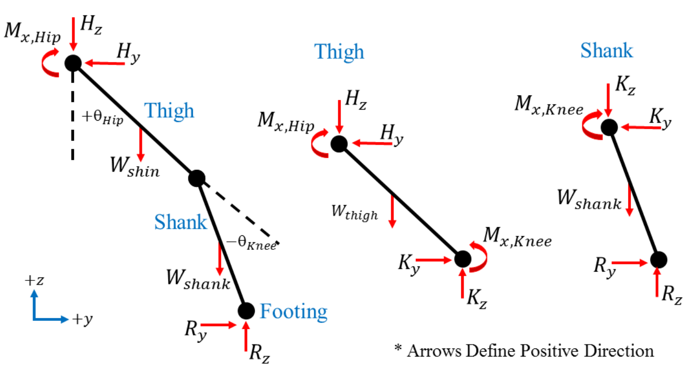

FIGURE 8. FREE-BODY DIAGRAM OF SINGLE LEG AND LIMBS.

initially assumed COM located at the center of each link. Friction and normal reaction forces (R_y, R_z) are applied at the footing of each leg.

The structural forces and moments of a single leg are detailed in Fig. 8. The external forces are replicated from the overall structure with the exception of the forces and torques at the hip. The hip forces (H_y, H_z) represent the distribution between each leg of the total loads at the hip, F_y and F_z. The torque applied at the hip ($M_{x,hip}$) is assumed to be zero with the objective of having actuation only necessary at the knee joint. This assumption is bolstered with subsequent analysis in Section 4.1. The equilibrium equations for the overall system and single leg are solved simultaneously with the objective of solving the torque at the knee ($M_{x,knee}$).

The static equilibrium equations for the overall system for a vertical weight at the hip of F_z can be determined from the diagrams in Fig. 7 as follows:

$$\sum F_Y = 0 = -F_y + R_{y,FL} + R_{y,RL} \tag{5}$$

$$\sum F_Z = 0 = -F_z + R_{z,FL} + R_{z,RL} - 2W_{thigh} - 2W_{shank} \tag{6}$$

$$\begin{aligned}\sum M_{x,h} = 0 = -M_{x,hip} + \overline{hr}_{FL} \times \begin{pmatrix} 0 \\ R_{y,FL} \\ R_{z,FL} \end{pmatrix} \\ + \overline{hr}_{RL} \times \begin{pmatrix} 0 \\ R_{y,RL} \\ R_{z,RL} \end{pmatrix} + \overline{hc}_{tFL} \times \begin{pmatrix} 0 \\ 0 \\ -W_{thigh} \end{pmatrix} \\ + \overline{hc}_{tRL} \times \begin{pmatrix} 0 \\ 0 \\ -W_{thigh} \end{pmatrix} \\ + \overline{hc}_{sFL} \times \begin{pmatrix} 0 \\ 0 \\ -W_{shank} \end{pmatrix} + \overline{hc}_{sRL} \times \begin{pmatrix} 0 \\ 0 \\ -W_{shank} \end{pmatrix}\end{aligned} \tag{7}$$

where $\overline{hr}_{FL}$ represents the position vector from the hip to the foot of the front leg (position labels are indicated in lowercase in Fig. 7).

The static equilibrium equations for the thigh in Fig. 8 are as follows:

$$\sum F_y = 0 = -H_y + K_y \tag{8}$$

$$\sum F_z = 0 = -H_Z + K_z - W_{thigh} \tag{9}$$

$$\begin{aligned}\sum M_{x,k} = 0 = -M_{x_{hip}} + M_{x_{knee}} \\ + \overline{hk} \times \begin{pmatrix} 0 \\ K_y \\ K_z \end{pmatrix} + \overline{hc}_{t,FL} \times \begin{pmatrix} 0 \\ 0 \\ -W_{thigh} \end{pmatrix}\end{aligned} \tag{10}$$

The static equilibrium equations for the shank illustrated in Fig. 8 are as follows:

$$\sum F_y = 0 = -K_y + R_y \tag{11}$$

$$\sum F_z = 0 = -K_z + R_z - W_{shank} \tag{12}$$

$$\begin{aligned}\sum M_{x,k} = 0 = -M_{x_{knee}} + \overline{kr} \times \begin{pmatrix} 0 \\ R_y \\ R_z \end{pmatrix} \\ + \overline{kc}_{s,FL} \times \begin{pmatrix} 0 \\ 0 \\ -W_{shank} \end{pmatrix}\end{aligned} \tag{13}$$

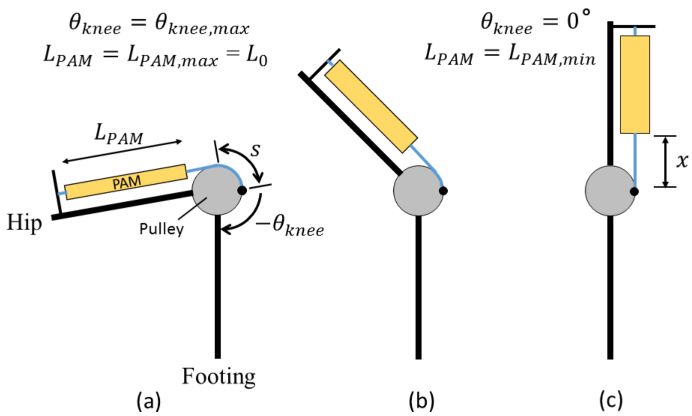

FIGURE 9. PAM ACTUATION OVER 100° ROM. (a) PAM AT MAX EXTENSION WITH θ_{knee}=$-100°$ (b) PAM AT INTERMEDIATE FORCE AND CONTRACTION (c) PAM FULLY CONTRACTED (θ_{knee}=0°)

Values for R_y, R_z, and $M_{x,knee}$ are all solved through the system of equations simultaneously. These values are found for every leg orientation (FL/RL) with the opposing leg (RL/FL) in the near and far orientations. The RL near and far orientations provide minimum and maximum values for the FL respectively for $M_{x,knee}$, R_y, and R_z.

3.4 Modeling of Basic Transmission Mechanism

A constant radius pulley will serve as the exemplary transmission mechanism used to test feasibility of PAM knee actuation. This scheme is used as a straightforward measure of concept feasibility because of the constant mechanical advantage (moment arm) it provides independent of θ_{knee}. This means that the ratio between $M_{x,knee}$ and the actuation force required from the PAM is equal to the radius of the pulley. Figure 9 illustrates the basic pulley scheme used. The PAM is mounted to the thigh link of the exoskeleton on one end, and is attached at the other end to the pulley through a flexible cable. The pulley is centered at the knee joint, and is fixed to the shank link of the exoskeleton. Therefore, the angle of rotation of the pulley (the angle between the longitudinal axes of the PAM and shank) is equal to θ_{knee}.

Overall, with the contraction and force requirements defined for every knee joint angle, the requirements for static equilibrium can then be compared to the force-contraction capabilities of the PAM as defined in Fig. 3.

3.4.1 Required Contraction of PAM To enable the rotation of the thigh link with respect to the knee joint, the PAM must provide the necessary actuation force for static equilibrium of the exoskeleton while also extending and contracting to compensate for the amount of cable in contact with the pulley. From the diagram in Fig. 9, the PAM must be in a state of free (maximum) contraction with $\theta_{knee} = 0$ (Fig. 9c). With increased flexion of the knee joint, the PAM elongates to compensate for the length of cable displaced through contact with the pulley (Fig. 9b). At the point of maximum rotation of the knee joint, the PAM is fully extended to its resting length, Ł$_0$ (block force condition) (Fig. 9a). This orientation demarcates the point at which the PAM cannot allow any additional rotation of the knee joint.

The change in length of cable that is in contact with the pulley, ds, as a function of the angle turned by the pulley, $d\theta$, is given by:

$$\int ds = \int_{\theta}^{\theta_{max}} r(\theta) d\theta \tag{14}$$

where the change in length of the PAM is equal to the change in cable length, and the angle of the pulley is determined by the knee joint angle. Therefore, for a constant radius pulley the change in length of the PAM is simply:

$$\Delta L_{PAM} = r_{pulley}(\theta_{max} - \theta) \tag{15}$$

where r_{pulley} is the radius of the pulley, and θ_{max} is the maximum knee joint angle. The PAM change in length compared to its resting length is the percent contraction of the PAM, and is defined as $\Delta L_{PAM}/L_0$.

3.4.2 Required PAM Actuation Force The constant radius pulley provides a constant moment arm at any degree of knee rotation to convert the PAM force to knee joint torque. The relationship between PAM force, F_{PAM}, and torque output, τ_{knee}, is given by:

$$F_{PAM} = \frac{\tau_{knee}}{r_{pulley}} \tag{16}$$

where r_{pulley} is the radius of the pulley.

With both the required torque ($M_{x,knee} = \tau_{knee}$) for each knee joint angle, and with a set pulley radius, the actuation force required from the PAM for each knee angle is defined.

4 ANALYSIS

With the kinematic model, feasible stances, static loading model, and basic transmission model covered in Section 3, analysis of the feasibility of PAM actuation of the knee joint can commence. The loading on the exoskeleton is analyzed first for all feasible stances, and then equilibrium knee torques are presented as a function of knee joint angle. From this, the basic pulley mechanism relations will be applied to translate the required knee torques with respective knee angles into actuation forces with respect to actuator contraction. Finally, if the required actuation forces fall within the characteristic force-contraction capabilities of the PAM, then PAM actuation of the FORTIS knee joint is shown to be feasible.

Table 2 lists all of the assumed external loads that act on the structure in their defined positive directions, and also gives the corresponding lengths (and adjustment ranges) of each link.

TABLE 2. FORTIS PARAMETERS USED FOR ANALYSIS.

Limb	Mass (kg)	Length/Range (cm)
pelvis	41.0	50
thigh	4.6	45.7 (41.9-51.4)
shank	2.3	50.8 (47.0-56.5)

4.1 Static Loading on FORTIS

The loading on the exoskeleton structure is now analyzed for the range of feasible stances using Eqs. (5- 13) with the applied loads and link lengths from Table 2. With the set FL orientation analysis ultimately resulting in values closer to the limits of PAM actuation, the shown figures will focus on these results.

The normal force R_z, friction force R_y, and knee torque $M_{x_{knee}}$ required for zero moment at the hip are shown in Fig. 10, Fig. 11, and Fig. 12, respectively. The areas outside of the colored regions indicate FL stances that are not feasible. Actuation of the hip joint would only be necessary if the friction required at the footings for equilibrium without hip actuation was an unrealistic value (coefficient of friction >1). To ensure that footing friction is sufficient, a value of zero hip torque ($M_{x,hip} = 0$) is applied to the equilibrium equations. The resulting maximum coefficient of friction value (COF=R_y/R_x) came out to be about 0.6 leaving it reasonable to conclude that a torque applied at the hip joint will not be necessary.

As a necessary tool for analysis, the knee torques for each FL orientation from Fig. 12 must be represented in a form that shows the relationship between the angle of the knee, and necessary torque for equilibrium in a given stance.

Since PAM contraction is a function of knee angle (Eq. (15)), and the PAM actuation force is a function of knee torque (Eq. (16)), then it is desired to convert the knee torque values with respect to FL orientations from Fig. 12 into torque values with respect to knee angle as provided in Fig. 13. This puts the required torque values in a form that can readily be converted to PAM actuation force as a function of PAM contraction. With the application of Eqs. (15) and (16), Fig. 13 is converted to PAM actuation force with respect to PAM contraction for comparison to the PAM's force-contraction capabilities.

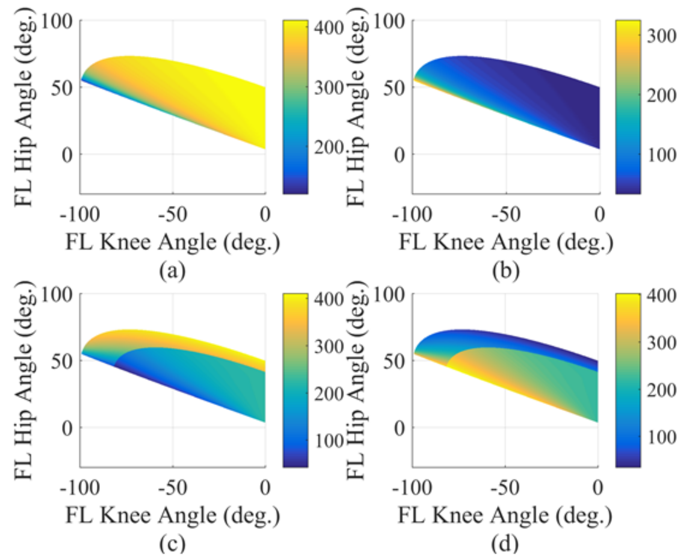

FIGURE 10. NORMAL FORCES (R_z) ON FOOTING FOR (a) RL-NEAR ORIENT. (b) FL-NEAR ORIENT. (c) RL-FAR ORIENT. (d) FL-FAR ORIENT.

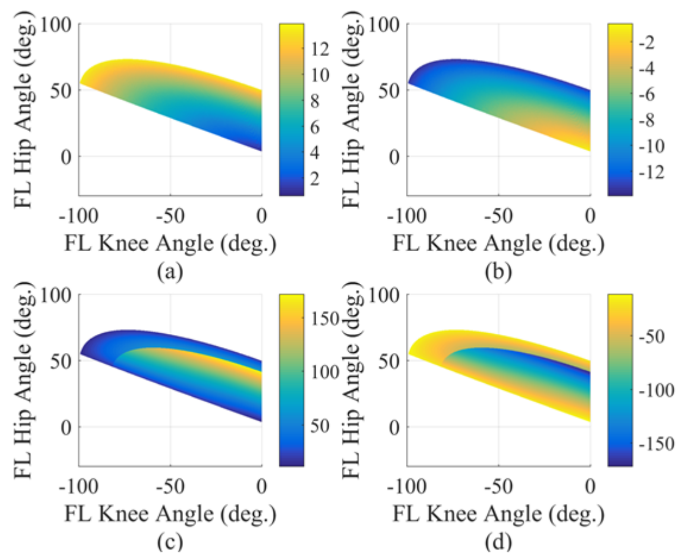

FIGURE 11. FRICTION FORCES (R_y) ON FOOTING FOR (a) RL-NEAR ORIENT. (b) FL-NEAR ORIENT. (c) RL-FAR ORIENT. (d) FL-FAR ORIENT.

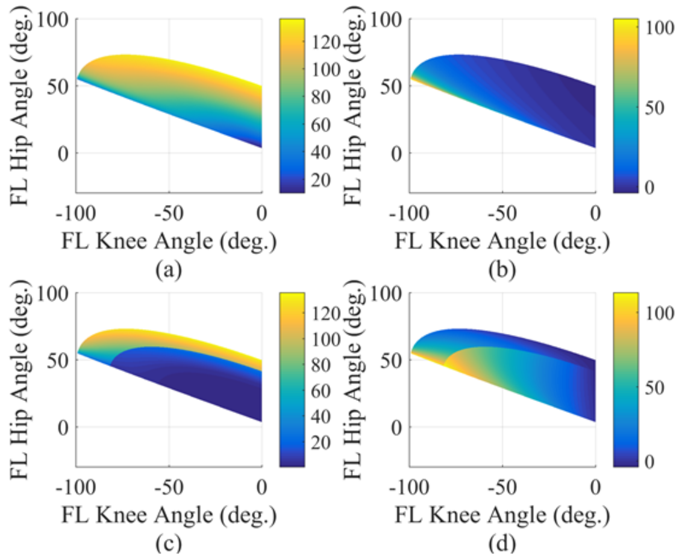

FIGURE 12. KNEE TORQUE ($M_{x,knee}$) FOR (a) RL-NEAR ORIENT. (b) FL-NEAR ORIENT. (c) RL-FAR ORIENT. (d) FL-FAR ORIENT.

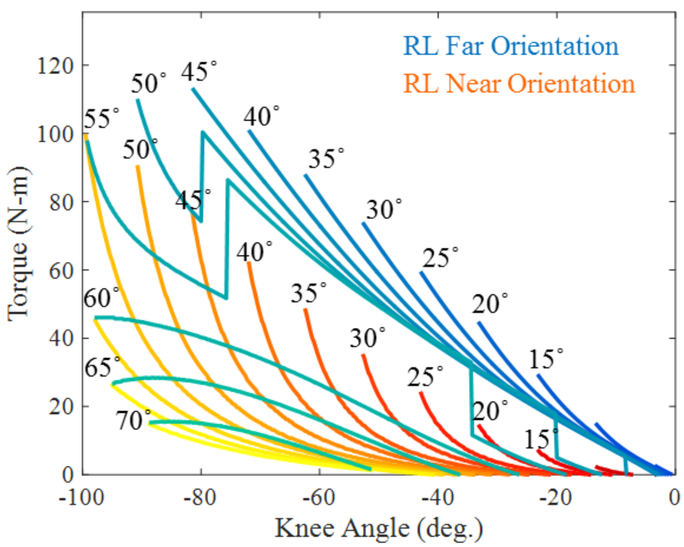

FIGURE 13. FRONT LEG KNEE TORQUE ($M_{x,knee}$) VERSUS KNEE ANGLE (θ_{knee}) FOR NEAR AND FAR ORIENTATIONS.

Figure. 13 represents the required stiffness of the knee joint with respect to constant FL θ_{hip} values. Each curve represents the required $M_{x_{knee}}$ for a constant θ_{hip} orientation of the FL with respect to varying FL θ_{knee} orientations. Therefore, these curves represent the same torque values as given in Fig. 12b and 12d, but in a transformed representation. The required torque curves

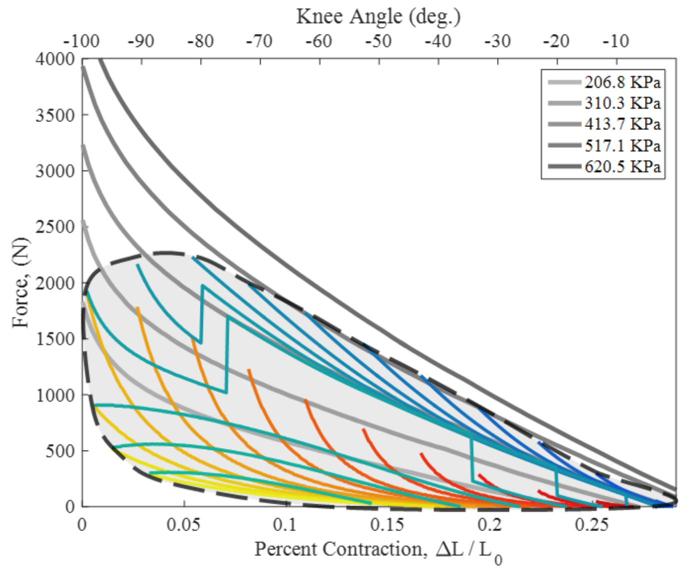

FIGURE 14. REQUIRED ACTUATION FORCE ENVELOPE (SHADED REGION) RELATIVE TO CAPABILITY OF PAM ACTUATOR

for the FL in both the RL near (red, from Fig. 12b) and far (blue, from Fig. 12d) boundary orientations are given. The near and far orientation curves of this plot represent the lower and upper bounds of the torques that can be experienced for each respective FL orientation. Therefore, for RL orientations that fall within the range defined by the near and far orientations, the torque experienced by the FL would be somewhere in the vertical space between the blue and red curves.

4.2 Feasibility of PAM Actuation

Fig. 14 overlays the required actuation force (converted from torque in Fig. 13 using Eq.(16)) onto the actuation capabilities of the given PAM (from Fig. 3). Required actuation force is given as a function of both FL knee angle (top x-axis) and PAM contraction (bottom x-axis), with the linear relationship between the two axes drawn from Eq.(15). A pulley radius of 5 cm is used with the 30 cm PAM previously introduced in Sec. 2.2. The boundary of the actuation stiffness curves represent an envelope of required actuation forces (shaded region within dashed line). With the resulting envelope not breaching the PAM's 620 kPa (90 psi) force-percent contraction threshold curve, actuation of the exoskeleton with the applied 30 cm PAM and 5 cm pulley is shown to be feasible for all attainable stance orientations.

Figure 14 also depicts how the nonlinearity of the required torque curves resemble the nonlinearity of the PAM's constant pressure curves. This is beneficial, because the closer the required force stays to a constant pressure curve, the less the pressure of the PAM needs to be adjusted to support the torque load.

In other words, if the required actuation force for static equilibrium were to move along one of the PAM's constant pressure curves, the PAM would be able to passively support the torque load without any additional pressure input necessary.

This analysis limited knee joint ROM to a maximum of 100° of flexion, and was caused by the limited PAM contraction available in conjunction with the transmission mechanism used. PAM contraction is limited by the minimal space on the exoskeleton thigh link, prohibiting the usage of a longer PAM. This ROM proved to be sufficient for all attainable stances, however this does slightly reduce the knee ROM of the FORTIS exoskeleton which may have unforseen effects.

5 CONCLUSIONS AND FUTURE WORK

This research examined the viability of adding PAM actuation to the FORTIS knee joint in an effort to support all feasible static stances that a user could assume during maintenance and manufacturing tasks. Computational models were developed to represent the kinematics, feasible stances, statics, and a basic transmission mechanism for the FORTIS. With defined boundaries of feasible leg orientations defined, and external loading on the FORTIS estimated, the range of possible forces and torques on the structure with respect to every feasible leg orientation was defined. Load analysis was presented only for the front leg with knowledge that the torques on the front leg would be the limiting factor.

The ranges of required stiffness for actuation of the knee joint were defined as a function of knee angle, enabling a direct comparison between the PAM's inherent force-contraction characteristics, and the required stiffness of the knee joint with respect to knee angle. A chosen pulley radius was used to define the force and contraction required of the PAM to actuate the knee. An envelope was drawn around all of the threshold actuation force values, and overlaid onto the force-contraction curves of the PAM for comparison. With this envelope constrained within the operational region of the PAM, feasibility of PAM actuation of the exoskeleton knee joint was displayed.

Future work on PAM actuation of the FORTIS will expand upon the analysis provided in this study. A prototype of the knee joint is being designed and fabricated, and will be used to experimentally validate the presented models and analysis. Alternative transmission mechanisms will also be analyzed that can transmit the required torque to the knee, while also maximizing the knee joint rotation for the constrained contraction length of the PAM.

Although assistance of static stances was the focus of this study, analysis of the dynamics of the exoskeleton should also be analyzed for walking and motions between stances. Although the additional weight and inertia from PAM actuation is minimal, dynamic analysis to complement that static analysis done in this study is essential to provide a full profile of the PAM actuated FORTIS exoskeleton.

ACKNOWLEDGMENT

The authors would like to acknowledge the Naval Air Systems Command which supported this research under Contract #N00421-13-2-M016. We would also like to thank our grant monitor, Greg Kennedy, for his generous advice and support.

REFERENCES

[1] Mone, G., 2008. "Building the real iron man". *Popular Science*, Apr.

[2] Zoss, A. B., and Kazerooni, H., 2006. "Biomechanical design of the berkeley lower extremity exoskeleton (bleex)". *IEEE/ASME Transactions on Mechatronics,* ***11***(2), Apr., pp. 128–138.

[3] Mattern, J. G., McArdle, D. G., and Ellis, D., 2013. "Industrial human augmentation systems for improved shipyard operations". In SNAME Annual Meeting and Ship Production Symposium, Society of Naval Architects and Marine Engineers.

[4] Shamaei, K., Napolitano, P. C., and Dollar, A. M., 2014. "Design and functional evaluation of a quasi-passive compliant stance control knee-ankle-foot orthosis". *IEEE Transactions on Neural Systems and Rehabilitation Engineering,* ***22***(2), Mar., pp. 258–268.

[5] Shamaei, K., Cenciarini, M., Adams, A. A., Gregorczyk, K. N., Schiffman, J. M., and Dollar, A. M., 2015. "Effects of exoskeletal stiffness in parallel with the knee on the motion of the human body center of mass during walking". In Proc. of the IEEE Intl. Conf. on Robotics and Automation, pp. 5557–5564.

[6] Yua, S., Hanb, C., and Choa, I., 2014. "Design considerations of a lower limb exoskeleton system to assist walking and load-carrying of infantry soldiers". *Applied Bionics and Biomechanics*(11), Mar., pp. 119–134.

[7] Beyl, P., Damme, M. V., Ham, R. V., Vanderborght, B., and Lefeber, D., 2009. "Design and control of a lower limb exoskeleton for robot-assisted gait training". *Applied Bionics and Biomechanics,* ***6***(2), pp. 229–243.

[8] Beyl, P., Knaepen, K., Duerinck, S., Damme, M. V., Vanderborght, B., Meeusen, R., and Lefeber, D., 2011. "Safe and compliant guidance by a powered knee exoskeleton for robot-assisted rehabilitation of gait". *Advanced Robotics,* ***25***, pp. 513–535.

[9] Kurz, T., 2003. *Stretching Scientifically: A Guide to Flexibility Training, 4th ed.* Stadon, Island Pond, Vermont, Mar.

[10] Robinson, R., Kothera, C., Woods, B., III, R. V., and Wereley, N., 2011. "High specific power actuators for robotic manipulators". *Journal of Intelligent Material Systems and Structures,* ***22***(13), pp. 1501–1511.